AAPS PharmSciTech, Vol. 13, No. 4, December 2012 (© 2012)
DOI: 10.1208/s12249-012-9832-1

Research Article

Characterisation of Ilomastat for Prolonged Ocular Drug Release

Gary Parkinson,[1] Simon Gaisford,[1] Qian Ru,[1,2] Alastair Lockwood,[1,2] Ashkan Khalili,[1,2] Rose Sheridan,[3] Peng T. Khaw,[2] Steve Brocchini,[1,2] and Hala M. Fadda[1,2,4,5]

Received 2 May 2012; accepted 24 July 2012; published online 18 August 2012

Abstract. We are developing tablet dosage forms for implantation directly into the subconjunctival space of the eye. The matrix metalloproteinase inhibitor, ilomastat, has previously been shown to be efficacious at suppressing scarring following glaucoma filtration surgery (GFS). We report on the physical characterisation of ilomastat which is being developed for ocular implantation. Since ilomastat is being considered for implantation it is necessary to examine its polymorphs and their influence on aspects of the *in vitro* drug release profile. X-ray powder diffraction identified two polymorphs of ilomastat from different commercial batches of the compound. Tablets were prepared from the two different polymorphs. Isothermal perfusion calorimetry was used to show that amorphous content is not increased during tablet formulation. The melting points of the two polymorphs are 188 and 208°C as determined by differential scanning calorimetry. Utilising single crystal X-ray diffraction, the structural conformations and packing arrangements of the different polymorphs were determined. The orthorhombic crystal crystallised as a monohydrate while the second monoclinic crystal form is non-solvated. Ilomastat tablets prepared from the two different solid forms exhibited similar drug release profiles *in vitro* under conditions mimicking the aqueous composition, volume and flow of the subconjunctival space after GFS. This suggests that a reproducible dose at each time point during release after implantation should be achievable *in vivo* with ilomastat tablets prepared from the two polymorphs identified.

KEY WORDS: ocular drug delivery; enantiotrope; dissolution; biorelevant media; solid–solid transition.

INTRODUCTION

Small molecular weight active ingredients commonly exhibit polymorphism and/or pseudo-polymorphism and may crystallise to different habits. This has very important implications because these different solid forms can display different physicochemical properties that impact drug development and performance. Hydrate forms often have very different physicochemical properties compared to the anhydrous crystals (1). Mechanical drug properties that may be influenced by differences in crystal habit, and which are important for the reproducible manufacture of dosage forms, include powder flow, compactibility and tensile strength (2). Performance parameters such as dissolution rate, bioavailability and stability can also be highly influenced by the crystal arrangements that the compound may adopt (3). In particular, implantable dosage forms that are designed for dissolution over several days require that that the polymorphic forms of the active ingredient be evaluated to ensure that reproducible performance can be maintained.

We are developing a dosage form of the matrix metalloproteinase inhibitor ilomastat (MW 388.5 g/mol; log P 0.9, pK_a 8.9; Fig. 1) that is designed for ocular implantation into the subconjunctival space after glaucoma filtration surgery (GFS) to create a pathway to drain aqueous humour from the eye (Fig. 2). This is to lower the eye pressure and prevent irreversible damage to the optic nerve. The major cause of failure in GFS is scarring around the drainage site leading to blockage and a rise in intraocular pressure. Glaucoma is the commonest cause of irreversible blindness in the world, and in many parts of the world the only practical solution is a successful operation. The only proven treatment in glaucoma is to decrease IOP so that optic nerve damage can be halted (4).

Current clinical practice to reduce scarring around the drainage site is to place a sponge soaked in a cytotoxic solution in the subconjunctival space for several minutes before completing the GFS procedure. Mitomycin-C and 5-fluorouracil are frequently used and although they have improved the outcome of GFS (5) they are associated with potentially blinding complications (6,7). Moreover, the use of a saturated sponge yields a solution that rapidly clears, necessitating repeated applications *via* injections into the subconjunctival tissue that are painful for the patient and impractical. The use of injections and solutions generally also result in high local concentrations of drug followed by rapid clearance by absorption into the conjunctiva.

[1] UCL School of Pharmacy, London, WC1N 1AX, UK.
[2] NIHR Biomedical Research Centre, Moorfields Eye Hospital and UCL Institute of Ophthalmology, London, EC1V 9EL, UK.
[3] Translational Research Office, UCL, London, WC1E 6BT, UK.
[4] Present address: Department of Pharmaceutical Sciences, College of Pharmacy and Health Sciences, Butler University, 4600 Sunset Avenue, Indianapolis, Indiana 46208, USA.
[5] To whom correspondence should be addressed. (e-mail: hfadda@butler.edu)

1530-9932/12/0400-1063/0 © 2012 American Association of Pharmaceutical Scientists

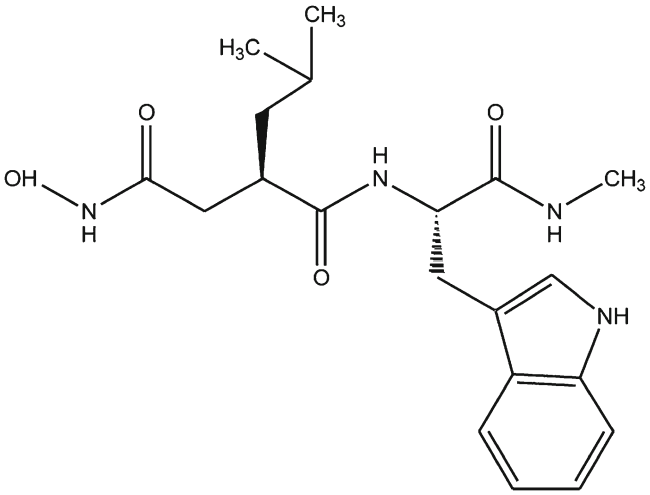

Fig. 1. Molecular structure of ilomastat

Currently, there are no licensed anti-fibrotic medicines for ocular use which might have a higher therapeutic index compared to the currently used cytotoxics. Our group has shown that ilomastat injections into the subconjunctival space in a clinically validated *in vivo* GFS model were found to significantly prolong survival of the bleb by reducing scarring while being safe and well tolerated (8). We are now focused on prolonging the local ocular pharmacokinetics of ilomastat within the subconjunctival space as this overcomes the need for multiple injections (9). We have been developing an implantable tablet dosage form designed to dissolve for periods of 3 to 4 weeks within the subconjunctival space (10) (Fig. 2). This is potentially very important as there are no licensed medicines for the prevention of scarring in the body or eye, even though there are many situations where antiscarring therapies are needed. Furthermore, several billion pounds have been spent on the development of MMP inhibitors with no licensed product, in part because of the side effects which appear to occur with cumulative doses above 1,600 mg. The expected dose of the tablet we are developing comprises only 2 mg of ilomastat, which is thought to be the amount necessary to provide local ocular sub-conjunctival drug release over a 3- to 4-week period. The study reported here focuses only on the *in vitro* aspects of the ilomastat tablet to determine what material changes may occur during dissolution.

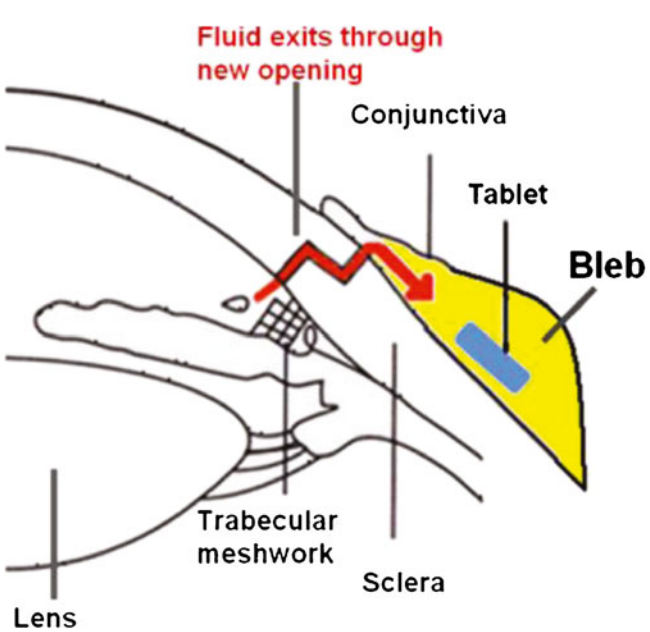

Fig. 2. A schematic diagram illustrating the positioning of ilomastat tablet into the sub-conjunctival space following glaucoma filtration surgery

Ilomastat is a typical hydroxamic acid derived matrix metalloproteinase inhibitor, whose properties are not dissimilar to several other MMP inhibitors. Furthermore, the ilomastat implantable tablet could easily be adapted for other situations in the human body where there is scarring including the eyelids, vitreous cavity, the abdominal cavity, joints and even the central nervous system (11–13). A key specification is that it must dissolve in a reproducible manner and this is assessed here using a flow cell designed to simulate the subconjunctival physiology; with particular attention to volume, aqueous flow rate and fluid composition. The subconjunctival space exists as an open flow system caused by anterior chamber aqueous drainage. The total volume of the bleb can range from about 50 to 200 μl. In healthy adult eyes, daytime mean aqueous humour flow is typically 2.2 to 3.1 μl/min (14). Here we compare the *in vitro* drug release profiles of ilomastat tablets prepared from different batches of the drug under simulated subconjunctival conditions. Furthermore, we identify the crystal forms of ilomastat in these different lots and solve their crystal structure. We also determine what changes in the physical forms of ilomastat may occur when the tablet is exposed to an aqueous environment for a prolonged period and how this affects *in vitro* performance.

MATERIALS AND METHODS

Materials

Three different batches of ilomastat were studied. Batch L9032752 (99.3% purity) and batch L9110405 (98.3% purity) from US Biological (MA, USA; batches 1 and 2, respectively) and batch 173-135-1 (99.15% purity) from Ryss (CA, USA; batch 3). We later show that batches 1 and 3 relate to polymorph 1 and batch 2 relates to polymorph 2 of ilomastat crystals. These will be hereafter referred to as polymorphs 1 and 2.

All salts to make up pH 7.4 phosphate-buffered saline (PBS) and HPLC buffer were of analytical grade and purchased from VWR (Leicestershire, UK). HPLC column used for the *in vitro* drug release quantification of ilomastat was a RP-C18 (Superlco Discovery column 88913–05).

Tablet Fabrication

Ilomastat tablets of different masses (1 or 2 mg) were prepared without excipients by direct compression (2 bar) using a hydraulic IR press (Specac, UK) and custom-made 2-mm punch and die sets (I Holland Ltd, Nottingham, UK). The same compression force was applied throughout the tablet manufacturing process. This was the minimum compression force required to fabricate ilomastat tablets that are robust and do not fragment on handling. Higher compression forces were found to retard the dissolution of ilomastat tablets. Drug release studies were performed on the 1 mg tablets with a thickness of 0.36±0.03 mm (mean ± SD).

Differential Scanning Calorimetry

Temperature-modulated differential scanning calorimetry (DSC) was employed (Q2000, TA instruments LLC, New Castle, USA) with an underlying heating rate of 2°C/min, modulation amplitude 1°C/min and modulation period of 60 s. Experiments were performed with ilomastat powder (ca. 1 mg) or whole tablets. Samples were encased in aluminium Tzero pans with non-hermetic lids and experiments were performed with an empty pan as a reference. The instrument was calibrated prior to use with a certified indium standard.

Isothermal Calorimetry

Gas perfusion isothermal calorimetry (IC, performed with a 2277 TAM, TA Instruments LLC) was used to evaluate the presence of any amorphous content in the ilomastat tablets. Whole ilomastat tablets (ca. 2 mg) were loaded into a stainless steel ampoule (4 ml total volume) and allowed to reach equilibrium at 25°C. The relative humidity (RH) of the perfusing gas (150 ml/h) was set to 0% for the first 10 h of each experiment. The RH was then cycled between 90 and 0% for 8-h periods until two wet–dry cycles had been completed. Data were recorded with the dedicated software package Digitam 4.1. The instrument was calibrated with the electrical substitution method prior to use and operated on an amplifier setting of 1,000 μW. The reference channel contained an empty stainless steel ampoule.

Dynamic Vapour Sorption

Dynamic vapour sorption (DVS; Surface Measurement Instruments, London, UK) was used to determine water uptake at different humidity levels. DVS allows a sample to be weighed during exposure to humidity at a specific temperature. Ilomastat tablets (2 mg) were weighed into a convex sample pan. To evaluate the moisture uptake of ilomastat tablets on exposure to the aqueous ocular environment, tablets were first exposed to 0% RH humidity for 5 h over which the loss in sample mass (due to water loss) had stabilised. Tablets were then exposed to 90% RH at 35°C until an equilibrium mass was achieved. In a separate experiment, ilomastat tablets were gradually exposed to an incremental increase in humidity levels. Humidity was increased from 25 to 75% at 10% increments each of 3 h duration at a temperature of 25°C.

X-ray Diffractometry

X-ray diffractometry experiments were all performed on an Oxford Diffraction, Xcalibur microfocus NovaT X-ray diffractometer, using CuK_{α} radiation. Powder X-ray diffraction experiments (XRD) were performed using transmission geometry at room temperature with samples sealed in capillary tubes and rotated about Phi over 360° at 0.5°/S. Powder XRD experiments were performed on both freshly prepared tablets and on tablets exposed to an aqueous environment. Tablets were exposed to an aqueous environment in the drug release cells for different lengths of time; 1 day, 1 week and 2 weeks. CCD image data were processed by CrystAlisPRO, which provided powder scattering data and plots. Single-crystal XRD experiments were performed to determine an atomic resolution crystal structure of ilomastat. Large rod-shaped crystals of ilomastat were grown from methanol by recrystallisation from polymorph 1 using the slow evaporation of a 2-mg/ml solution at 4°C. Data were collected at 105 K on a single flash-frozen crystal processed and scaled using CrystAlisPRO. The crystals were assigned to space group $P2_12_12_1$, with unit cell dimensions a=4.9825 (5), b=19.0075 (14), c=22.5432 (10) Å, $\alpha=\beta=\gamma=90°$. The structure was solved by direct methods using SIR92 (15) and refined using SHELXL97 (16) from 3,778 independent reflections. All non-hydrogen atoms were refined by full-matrix, least squares with anisotropic temperature factors, with hydrogen atoms positioned using normal geometry. Ilomastat obtained from US Biological (batch 2) was crystalline and a single crystal was selected and characterised using XRD. The crystals were frozen (105 K), data were collected, and the space group was assigned to monoclinic $P2_1$ with unit cell dimensions a=11.534 (2), b=4.8940 (11), c=17.719 (6) Å, $\alpha=\gamma=90°$ β=95.96 (3)° giving rise to a new polymorph. The structure solved by direct methods SIR92 and refined using SHELXL97. Hydrogen atoms excluded from the refinement and all non-hydrogen atoms were refined by full-matrix, least squares methods with anisotropic temperature factors.

In Vitro Drug Release Studies and Solubility Measurements

Drug release studies were performed in an in-house designed 200-μl cell with an open flow system (Fig. 3). The rate of media flow through the cell was 2 μl/min to simulate typical flow of aqueous humour (14). Drug release experiments were performed at 35.5°C to mimic the temperature of the sub-conjunctival space (17). To better simulate the physiological environment of the sub-conjunctival space, the media chosen to circulate through the cells was Balanced Salt Solution (BSS Plus®; Alcon, Texas, USA). This solution contains various minerals and is enriched with bicarbonate, dextrose and amino acids. It closely simulates the aqueous humour and is used as an irrigating solution for intraocular surgical procedures. BSS Plus however presents a nutritious environment for microbial growth and it was therefore necessary to use 0.05% sodium azide as a preservative. Drug release in this complex medium was compared to (PBS), which is conventionally used in drug release studies. Both media were maintained at a pH of 7.4. Samples flowing out of the cell were analysed by HPLC for drug quantification. The mobile phase comprised 25% acetonitrile and 75% buffer (0.0135 M ammonium acetate, 0.6% triethylamine adjusted to pH 5.0±0.1 with acetic acid). A reverse phase C18 column was utilised at 40°C,

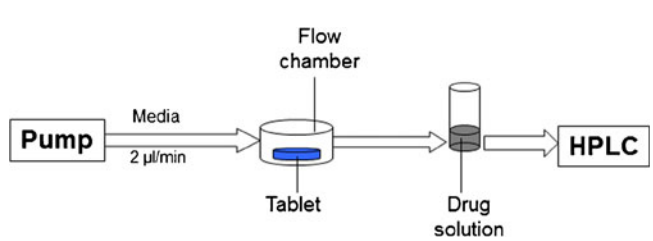

Fig. 3. A schematic diagram illustrating the open flow system designed to test *in-vitro* drug release under conditions simulating the subconjunctival space

flow rate of 1 ml/min, stop time 12 min, injection volume 10 μl and UV detection of 280 nm. This method differentiates between the diastereomeric degradants of ilomastat and its diastereomers. An integrated HP 1050 series HPLC system comprising an HP1050 autosampler, HP 1050 pump and HP 1050 UV–vis spectrophotometric detector was employed. The detector was interfaced with a PC with PC/Chrom+Software (H&A Scientific Inc., Greenville, NC). All drug release studies were run in triplicate.

Solubility of ilomastat polymorph 1 was measured in BSS Plus using the shake flask method. Excess drug was added to the solvent media and placed in a shaking water bath at 35.5°C for 24 h. The drug suspension was then filtered and aliquots of the resultant filtrate subjected to the appropriate dilution and analysed by HPLC.

RESULTS AND DISCUSSION

In this study we used three batches of ilomastat from two different commercial sources. Three different polymorphs of ilomastat were identified. Two of these polymorphs were identified from the different batches studied. One of these polymorphs undergoes a solid–solid transition to produce the third identified polymorph. The two polymorphs originating from the different ilomastat batches are easily discriminated by their diffraction patterns (Fig. 4). The onset of melting was determined to be 208°C for polymorph 1 (Fig. 5) and 188°C for polymorph 2. Further physical characterisation studies were performed on polymorph 1 due to its more abundant availability. No significant difference between the melting point of ilomastat powder as supplied and that of the tablet was observed. It is possible, however, that some change in physical form, typically to an amorphous matrix, can occur upon compression and it was decided to use isothermal calorimetry to determine if this was the case here. Results from isothermal perfusion calorimetry are illustrated in Fig. 6. The trace can be divided into five sections, corresponding to the five RH periods noted earlier:

1. Drying cycle allowing the sample to reach equilibrium
2. Exposure of the tablet to 90% RH; here the tablet exhibits an exothermic response which represents wetting of the ampoule, wetting of the tablet and (possibly) water uptake and crystallisation of any amorphous regions
3. Exposure of the tablet to 0% RH; here the tablet exhibits an endothermic response corresponding to drying of the ampoule, drying of the tablet and loss of any water taken up by the sample
4. Exposure of the tablet to a further cycle of 90% RH
5. Exposure of the tablet to a further drying cycle

If the tablet contained any amorphous fraction post compression then exposure to elevated humidity should cause recrystallisation to a crystal form. This event would proceed with a concomitant release of heat. Since crystallisation is irreversible, further wetting and drying should not induce any molecular disorder in the sample; thus it would be expected that the area of the first wetting event would be larger than that of the second. The areas of the two exothermic wetting peaks obtained are 335.35±2.9 and 335.6±4.38 mJ, respectively. This remarkable similarity between the two areas suggests that no amorphous regions were formed during tablet compression since the sensitivity of gas perfusion calorimetry for detecting amorphous contents in low molecular weight organic compounds is typically in the order of 0.5% (18,19). Interestingly, the shape of the first wetting peak is different from the shape of the second wetting peak and both wetting peaks differ in shape from the drying peaks. This suggests a possible change in the wetting kinetics of the tablet during each phase, possibly due to formation of a hydrate under high humidities and formation of an anhydrous form under low humidities.

Dynamic vapour sorption experiments (DVS) showed 4.1±0.63% water uptake of the dehydrated ilomastat tablets on exposure to 90% RH and complete elimination of all absorbed moisture on restoration to 0% RH levels. The molar ratio of water uptake to ilomastat is 1.07 to 1 moles. This provides circumstantial evidence for the formation of a monohydrate crystal. The rates of dehydration and rehydration observed were rapid, and these are largely determined by the size of the water channels and the strength of the hydrogen-bonding interactions that bind the water molecules in the

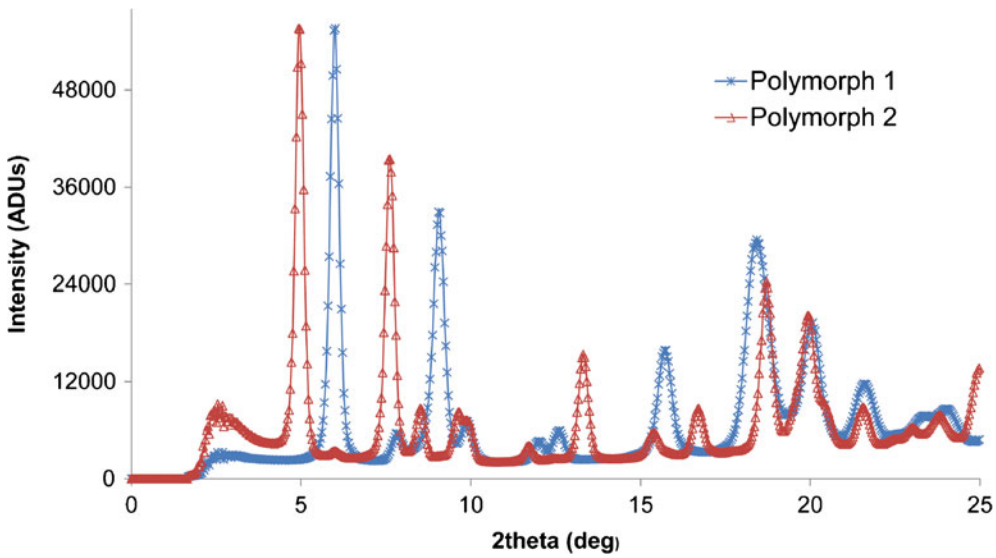

Fig. 4. X-ray powder diffractograms of the different ilomastat polymorphs

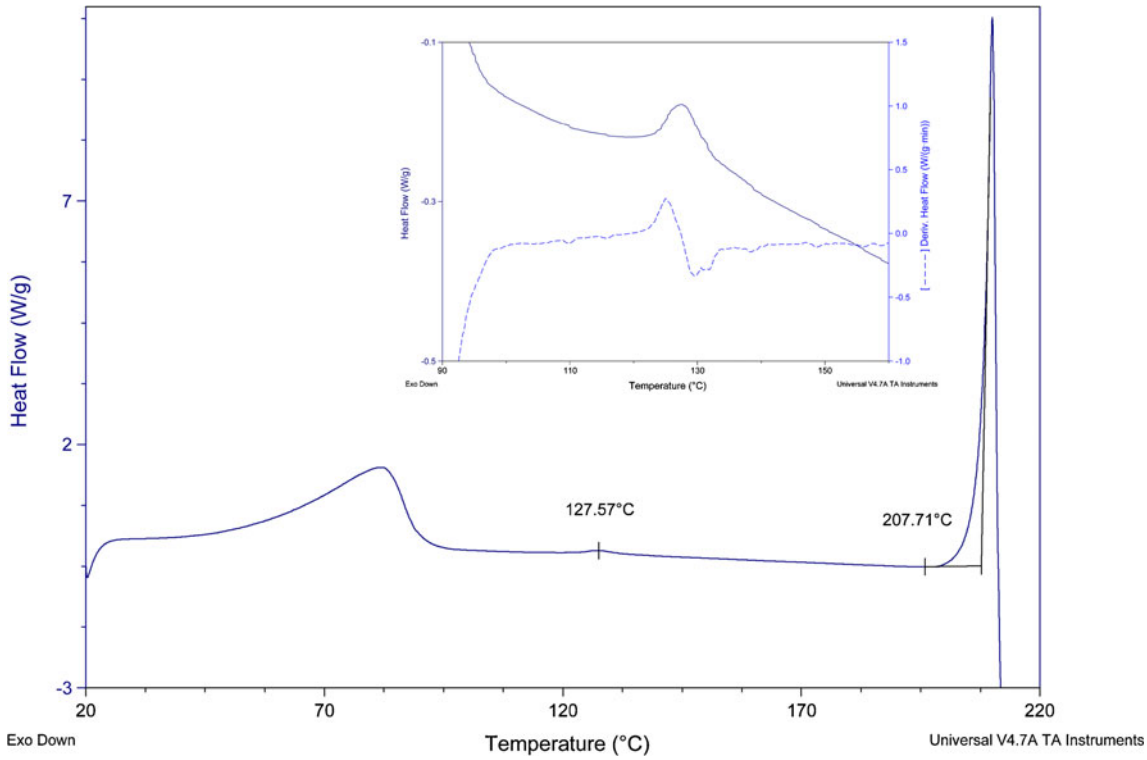

Fig. 5. DSC thermogram of ilomastat tablets formed from polymorph 1. Endothermic peak at 80°C represents dehydration. *Inset* illustrates the solid–solid transition observed at 128°C as a function of heat flow and the derivative of the heat flow

channels (20). Similar levels of water uptake are also observed on exposure to humidity levels ranging from 25 to 75% RH following dehydration of the tablet. If between 25 and 75% RH, at 25°C the water uptake is greater than 0.5% then hydrate formation is possible (21). A value of 0.5% (*w*/*w*) water or less is taken to represent up to three monolayers of

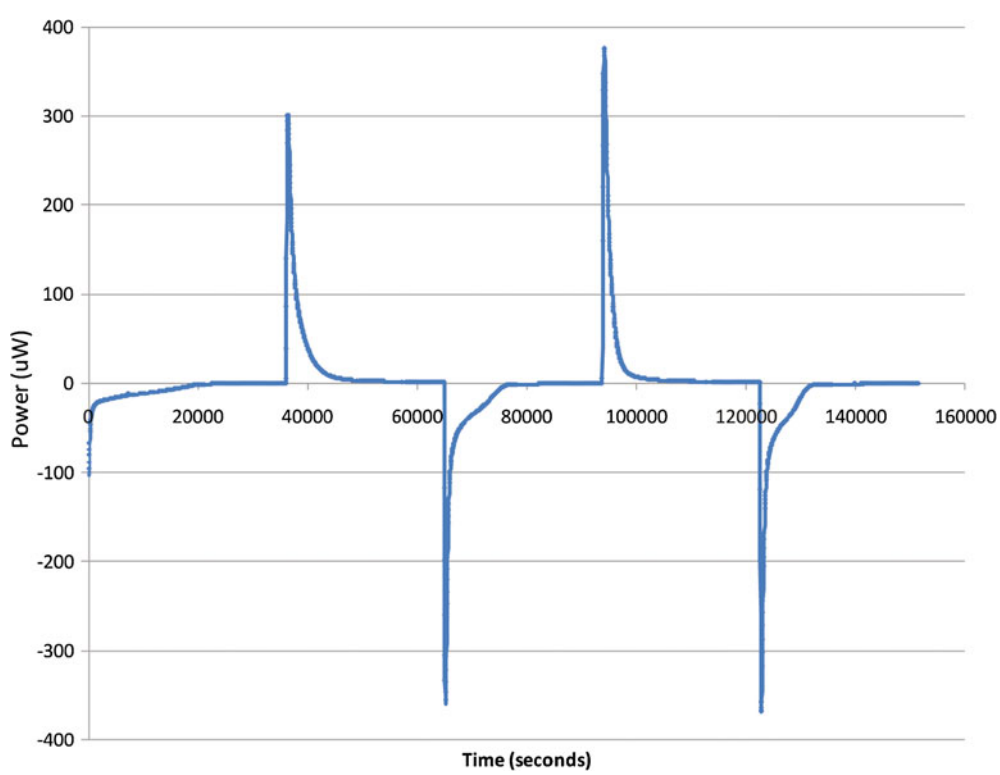

Fig. 6. Power–time response for the interaction of water with ilomastat tablet formed from polymorph 1 as obtained from isothermal perfusion calorimetry

adsorbed water on a typical crystalline pharmaceutical solid surface (21).

DSC scans of ilomastat tablets prepared from polymorph 1 showed a reversible, endothermic transition at 128°C (Fig. 5). Repeated heating (up to temperatures below the melt) and cooling cycles always showed the presence of this endothermic transition in the reversible heating signal of the modulated DSC scan. To determine if this is a solid–solid transition, the ilomastat tablet was heated to 150°C and X-ray diffraction (at ambient conditions) was performed on the heated tablet to determine if it exists in a different crystal form to the tablet at room temperature. The crystals of the heated tablet exhibited a different diffraction pattern to the ilomastat crystals at room temperature (Fig. 7). New diffraction peaks consistently appeared at 13 and 17 at 2θ (°) and shoulders at 8.5 and 19.5 2θ (°). A simple analysis of the new powder pattern profile, based on peak scattering positions and relative intensities, rules out the possibility of it being a mixture of polymorphs 1 and 2. We believe this provides evidence for an enantiotropic, solid–solid transition. Thus, a third polymorph of ilomastat is identified here. Although the tablet was heated to 150°C, X-ray powder diffraction was performed under ambient conditions and therefore the temperature of the tablet is likely to be below this while the X-ray scan was being performed. Despite this, a new polymorph was still detected since kinetics is an important factor in polymorphic transformations. In enantiotropic systems, different polymorphs are stable at different temperatures and pressures. One form is the stable one below the transition point while the other form is the stable form above the transition point. An energy barrier needs to be overcome to transform from one form to the other. This energy barrier may be reduced by moisture, impurities and excipients in the formulation. Seeds of the other crystal form may also be present which can accelerate transformation (22).

Rod-shaped crystals of ilomastat were grown in methanol (Fig. 8). These exhibit the same crystal form as polymorph 1. Crystallographic data and details of the single-crystal data collection are given in Table I. This polymorph is orthorhombic and four water molecules are present in the unit cell coordinated as a monohydrate (Fig. 9a). The other polymorph identified is a non-solvated monoclinic crystal (Table I). Ilomastat molecules are chiral and have an inherent flexibility. In the hydrated crystal, water is altering and stabilising the crystal geometry by changing the packing environment. Average distances of 2.84 Å exist between water and ilomastat molecules; which is representative of the length of a hydrogen bond. For the monoclinic crystal form, average bond lengths of 3 Å exist between the molecules in adjacent unit cells (Fig. 9b); which is also indicative of hydrogen bonds between ilomastat molecules.

Utilising single crystal data of the two different polymorphs we have generated theoretical powder diffraction patterns. The theoretical powder diffraction patterns for the orthorhombic and monoclinic crystals are in very good agreement with the experimental diffraction patterns obtained from batches 1 and 2, respectively. This indicates that there is no apparent contribution from other crystals in the batches studied.

Powder X-ray diffraction was performed on freshly prepared tablets prepared from polymorph 1 and tablets exposed to the aqueous environment of the cell for different periods of time. No changes were observed in the powder diffraction patterns on exposure to fluid. The absence of a change in the crystal lattice of the orthorhombic crystal indicates that a change in the dissolution profile of the tablet will not be observed during the course of release in the subconjunctival bleb. Moreover, if the monoclinic crystal undergoes hydrate formation on exposure to aqueous media this is likely to be immediate as illustrated by the DVS pattern of the dehydrated orthorhombic form. Therefore a deviation in the dissolution profile or sudden change in the dissolution rate over the course of drug release is unlikely to be observed.

The solubility of polymorph 1 of ilomastat in balanced salt solution was determined to be 415.6±68.2 μM. The drug release patterns of ilomastat tablets, prepared from polymorph 1, in BSS reveal an almost first order decline in drug concentration in the chamber with time (Fig. 10). The flow rate of dissolution media is constant at 2 μl/min; however, as time progresses, the driving force for dissolution decreases due to the increase in drug concentration in the bulk. This, coupled with the decline in tablet size and therefore absolute

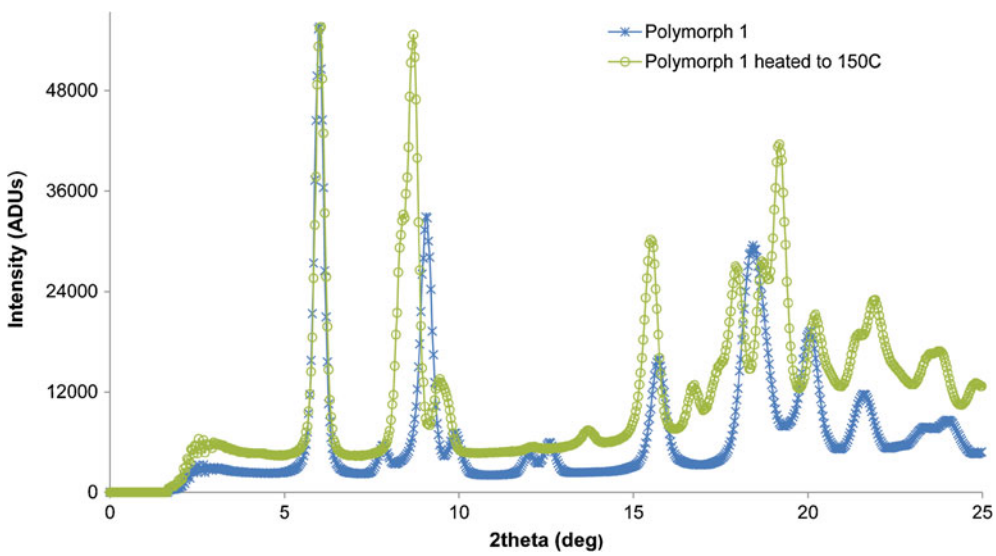

Fig. 7. Comparison of X-ray powder diffractograms of ilomastat enantiotropes

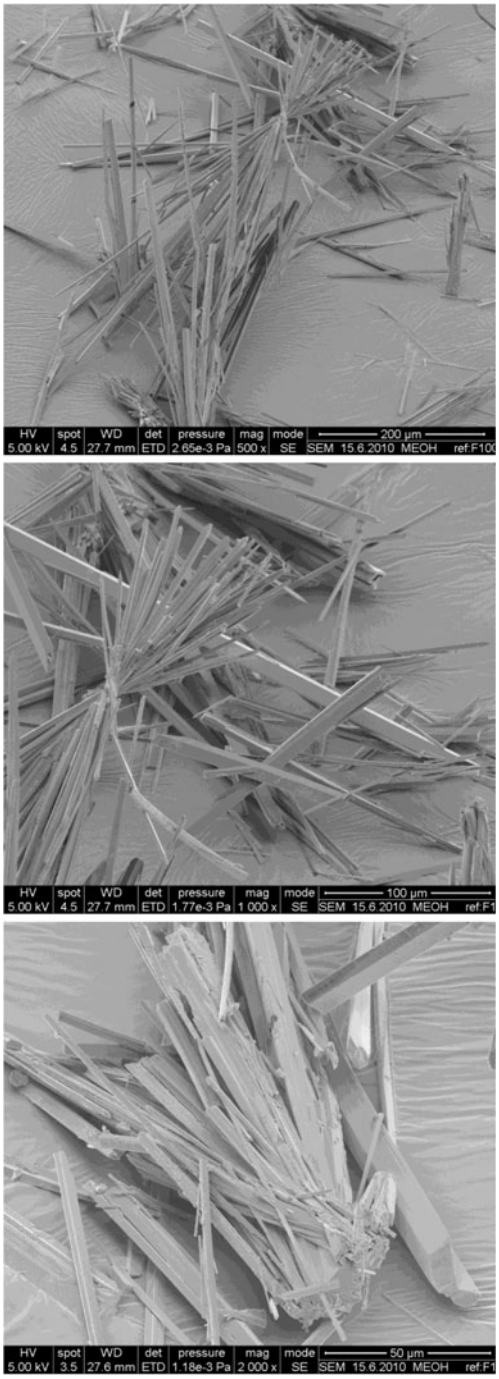

Fig. 8. Scanning electron microscopy images of orthorhombic ilomastat crystals (different magnifications are shown)

surface area, results in the observed decrease in drug concentrations over time. Interestingly, the release medium composition largely influences the drug concentrations observed with up to 1.4-fold differences in drug levels attained in BSS compared to PBS (Fig. 11). Ilomastat is an ionisable drug and its solubility is affected by the composition of ions and buffer species in the dissolution media (23–25). Nevertheless, under both release conditions the drug levels in the flow cell were above the IC_{50} of ilomastat for 2 weeks and complete tablet dissolution was achieved within 3 weeks. Ilomastat is a potent drug; the IC_{50} for the inhibition of matrix metalloproteinases

Table I. Crystal Data, Data Collection and Structure Refinement for Ilomastat Orthorhombic Monohydrate and Monoclinic Anhydrous Crystals

Parameter	Polymorph 1	Polymorph 2
Chemical formula	$C_{20}H_{28}N_4O_4{\cdot}H_2O$	$C_{20}H_{28}N_4O_4$
Molecular weight	388.46+18	388.46
Crystal system	Orthorhombic	Monoclinic
Space group	$P2_12_12_1$	$P2_1$
a/Å	4.9825 (3)	11.534 (2)
b/Å	19.0075 (14)	4.8940 (11)
c/Å	22.5432 (10)	17.719 (6)
α/Å	90	90
β/Å	90	95.96 (3)
γ/Å	90	90
V/Å^3	2,135.0 (5)	994.7 (6)
Reflection measured	3,864	1,854
Reflection unique	1,982	1,425
R(int)	0.04	0.093
Mean F^2/Sig F^2	23.97	17.27
Redundancy	1.9	1.3
Refinement ($4\sigma(I)$) F^2		
R_all (obs)	0.0613, 0.078	0.102, 0.123
wR2_obs	0.1778	0.2664
GOF	0.997	1.094
max, min Δρ/e Å^{-3}	0.467, −0.416	0.442, −0.350
Resolution Å	0.87	0.98
Temperature K	105	105
Z	2	4

present during fibrosis is ~30 μM as measured by matrix contraction assays (26,27). In this *in vitro* release study we have attempted to simulate various aspects of the subconjunctival space; however, several limitations to this *in vitro* model do exist. While 2 μl/min is the typical trabecular outflow into

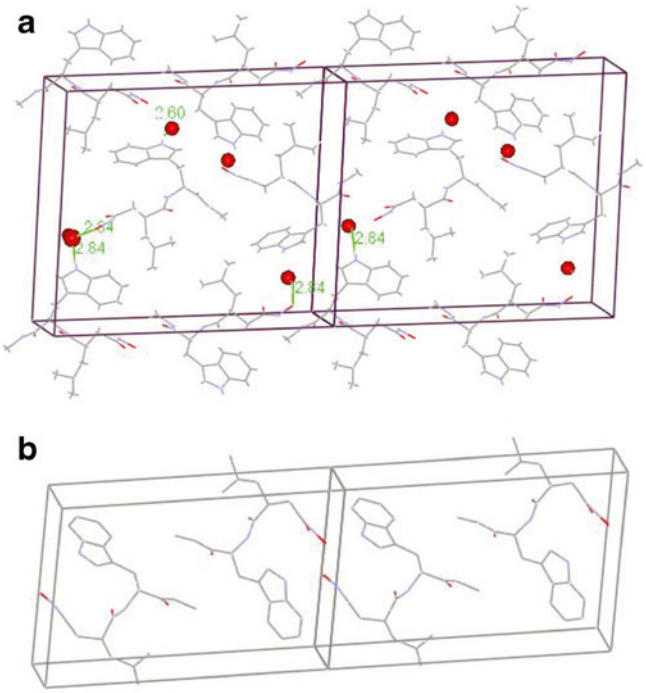

Fig. 9. **a** Crystal packing of orthorhombic 1*1*2 unit cell. **b** Crystal packing of monoclinic 1*1*2 unit cell

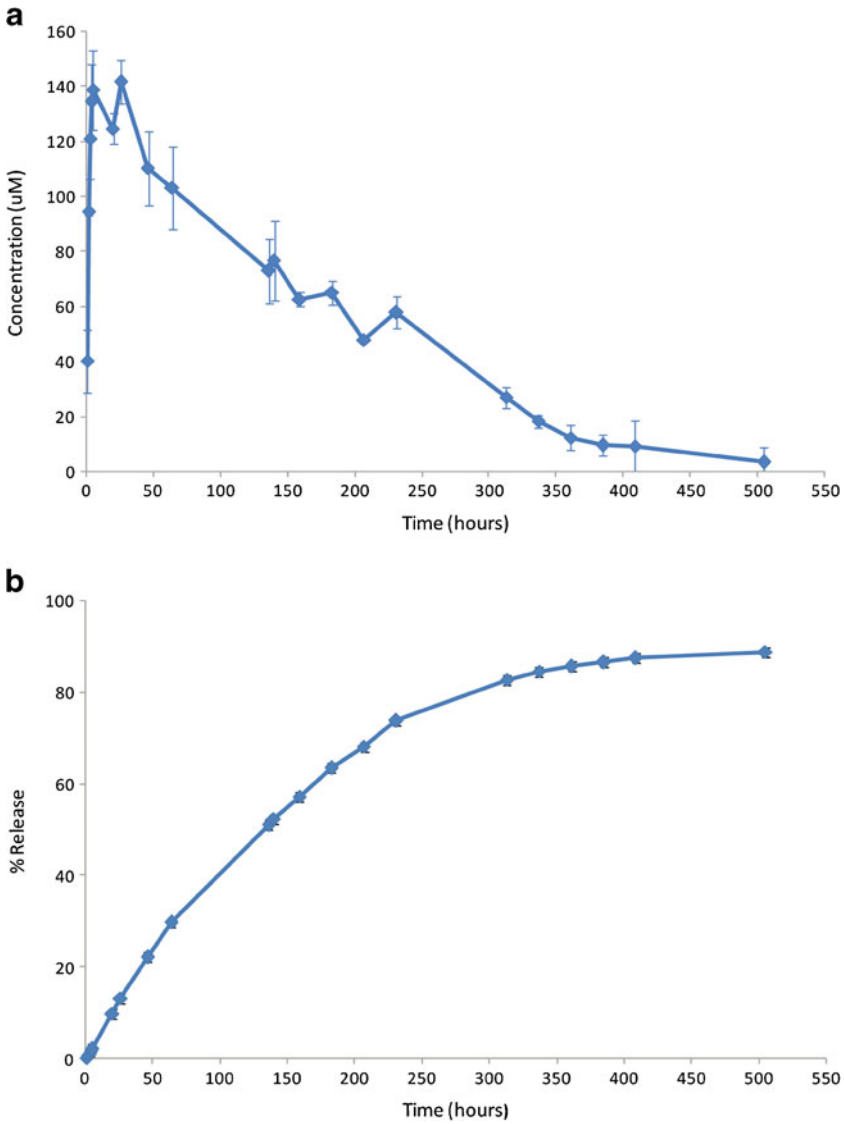

Fig. 10. *In-vitro* release of ilomastat 1 mg tablets, prepared from polymorph 1, in BSS plus buffer at 35.5°C, flow rate 2 μl/min. **a** Illustrates the concentration of ilomastat and **b** illustrates the cumulative release over time

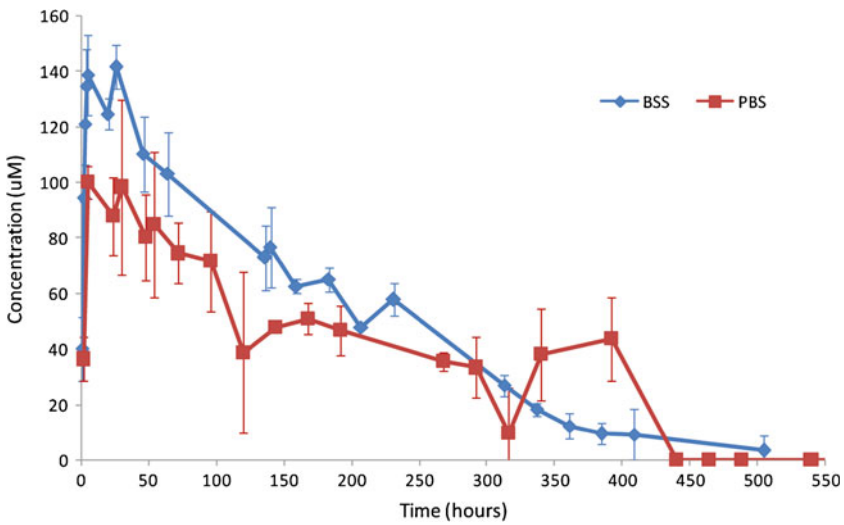

Fig. 11. Comparison of *in-vitro* release profiles of ilomastat tablets prepared from polymorph 1, in BSS and PBS media at 35.5°C, flow rate 2 μl/min

the subconjunctival space, this number is subject to diurnal and inter-individual variations. Furthermore, the bleb does not exist as one fluid chamber; however, it exists almost as a 'sponge' with fluid pockets interdispersed amongst a network of tissue and capillaries. This model can successfully discriminate between ilomastat tablets of different surface area and composition (data not shown) and is therefore currently being utilised for *in vitro–in vivo* correlation studies.

Drug polymorphs can exhibit different intrinsic dissolution patterns, which may have an influence on drug bioavailability and efficacy (28,29). In oral formulations, chloramphenicol palmitate polymorphs expressed different solubilities and dissolution rates, which were shown to affect drug absorption and plasma drug levels (28). In another study with sulfameter, the rate of gastrointestinal drug absorption was also shown to be different between different polymorphs (30). The release profiles of ilomastat tablets prepared from different solid forms were compared in the flow cell model. Insignificant differences were observed under the conditions simulating the subconjunctival bleb over the course of the study (ANOVA, post-hoc, $p>0.05$). This similarity in drug release may arise from the monoclinic crystal undergoing immediate hydration and conversion to the orthorhombic crystal on exposure to aqueous media. Alternatively, it may be attributable to similarities in the solubility of the two polymorphs.

CONCLUSIONS

The development of ilomastat as a non-cytotoxic anti-scarring agent for implantation into the sub-conjunctival space after glaucoma filtration surgery has required the characterisation of the crystalline forms of this molecule in a tableted dosage form. Two commercially available sources of ilomastat were used which displayed two polymorphic forms of ilomastat. Analysis of these solid crystalline forms by small molecule X-ray crystallography has identified an orthorhombic form with four water molecules present in the unit cell coordinated as a monohydrate and an anhydrous monoclinic form within a commensurately smaller asymmetric. The orthorhombic form of ilomastat also displays an enantiotropic, solid–solid transition at 128°C; thus revealing a third polymorph of ilomastat. Ilomastat tablets derived from polymorphs 1 or 2 have been successfully formed by direct compression without the inclusion of excipients or alteration of crystalline form. Isothermal calorimetry showed that no quantifiable amorphous regions were induced upon tablet compression. Furthermore, tablets prepared from the two solid forms exhibited similar drug release behaviour in conditions mimicking the subconjunctival bleb. Importantly, no materials changes in ilomastat arose that adversely affect its dissolution rate for its potential use as an active agent in an ocular implant in the subconjunctival space.

ACKNOWLEDGEMENTS

This research was supported by the Freemasons Grand Charity and was also supported in part by the Medical Research Council Developmental Pathway Funding Scheme (G801650), The Dorothy Hodgkins DHPA Scheme, The Helen Hamlyn Trust in memory of Paul Hamlyn, Fight for Sight, Moorfields Special Trustees, the Michael and Ilse Katz Foundation and the National Institute for Health Biomedical Research Centre at Moorfields Eye Hospital and the UCL Institute of Ophthalmology. The authors would like to thank Dr. Hardyal Gill for help with the HPLC method development of ilomastat. The scientific discussions with Dr. Aktham Aburub are gratefully acknowledged. The support and help of Mrs. Peggy Khaw in the preparation of this manuscript is much appreciated.

REFERENCES

1. Pudipeddi M, Serajuddin ATM. Trends in solubility of polymorphs. J Pharm Sci. 2005;94(5):929–39.
2. Datta S, Grant DJW. Crystal structures of drugs: advances in determination, prediction and engineering. Nat Rev Drug Discov. 2004;3(1):42–57.
3. Giron D, Goldbronn C, Mutz M, Pfeffer S, Piechon P, Schwab P. Solid state characterizations of pharmaceutical hydrates. J Therm Anal Calorim. 2002;68(2):453–65.
4. Weinreb RN, Khaw PT. Primary open-angle glaucoma. Lancet. 2004;363(9422):1711–20. Epub 2004/05/26.
5. Reynolds AC, Skuta GL, Monlux R, Johnson J. Management of blebitis by members of the American Glaucoma Society: a survey. J Glaucoma. 2001;10(4):340–7.
6. Parrish R, Minckler D. "Late endophthalmitis"—filtering surgery time bomb? Ophthalmology. 1996;103(8):1167–8.
7. Georgoulas S, Dahlmann-Noor A, Brocchini S, Khaw PT. Modulation of wound healing during and after glaucoma surgery. Glaucoma: an open window in to neurodegeneration and neuroprotection. Prog Brain Res. 2008;173:237–54.
8. Wong TTL, Mead AL, Khaw PT. Matrix metalloproteinase inhibition modulates postoperative scarring after experimental glaucoma filtration surgery. Investig Ophthalmol Vis Sci. 2003;44 (3):1097–103.
9. Wong TT, Mead AL, Khaw PT. Prolonged antiscarring effects of ilomastat and MMC after experimental glaucoma filtration surgery. Investig Ophthalmol Vis Sci. 2005;46(6):2018–22. Epub 2005/05/26.
10. Georgoulas S, Ru Q, Brocchini S, Khaw P. A novel single application prolonged release MMP inhibitor is superior to mitomycin in preventing scarring after experimental glaucoma surgery. Investig Ophthalmol Vis Sci. 2008;49:A4538.
11. Sheridan CM, Occleston NL, Hiscott P, Kon CH, Khaw PT, Grierson I. Matrix metalloproteinases: a role in the contraction of vitreo-retinal scar tissue. Am J Pathol. 2001;159(4):1555–66. Epub 2001/10/05.
12. Townley WA, Cambrey AD, Khaw PT, Grobbelaar AO. The role of an MMP inhibitor in the regulation of mechanical tension by Dupuytren's disease fibroblasts. J Hand Surg Eur Vol. 2009;34 (6):783–7. Epub 2009/09/30.
13. Brochhausen C, Schmitt VH, Rajab TK, Planck CN, Kramer B, Wallwiener M, *et al*. Intraperitoneal adhesions—an ongoing challenge between biomedical engineering and the life sciences. J Biomed Mater Res A. 2011;98(1):143–56. Epub 2011/05/07.
14. McLaren JW. Measurement of aqueous humor flow. Exp Eye Res. 2009;88(4):641–7.
15. Altomare A, Cascarano G, Giacovazzo C, Guagliardi A. Completion and refinement of crystal-structures with Sir92. J Appl Crystallogr. 1993;26:343–50.
16. Sheldrick GM, Schneider TR. SHELXL: high-resolution refinement. Macromol Crystallogr Part B. 1997;277:319–43.
17. Kawasaki S, Mizoue S, Yamaguchi M, Shiraishi A, Zheng X, Hayashi Y, *et al*. Evaluation of filtering bleb function by thermography. Br J Ophthalmol. 2009;93(10):1331–6.
18. Mackin L, Zanon R, Park JM, Foster K, Opalenik H, Demonte M. Quantification of low levels (<10%) of amorphous content in micronised active batches using dynamic vapour sorption and isothermal microcalorimetry. Int J Pharm. 2002;231(2):227–36.

19. Gaisford S, Dennison M, Tawfik M, Jones MD. Following mechanical activation of salbutamol sulphate during ball-milling with isothermal calorimetry. Int J Pharm. 2010;393(1–2):74–8.
20. Vippagunta SR, Brittain HG, Grant DJW. Crystalline solids. Adv Drug Deliv Rev. 2001;48(1):3–26.
21. Newman AW, Reutzel-Edens SM, Zografi G. Characterization of the "Hygroscopic" properties of active pharmaceutical ingredients. J Pharm Sci. 2008;97(3):1047–59.
22. Barbas R, Marti F, Prohens R, Puigjaner C. Polymorphism of norfloxacin: evidence of the enantiotropic relationship between polymorphs A and B. Cryst Growth Des. 2006;6(6):1463–7.
23. Fadda HM, Sousa T, Carlsson AS, Abrahamsson B, Williams JC, Kumar D, *et al*. Drug solubility in luminal fluids from different regions of the small and large intestine of humans. Mol Pharm. 2010;7(5):1527–32.
24. Fadda HM, Basit AW. Dissolution of pH responsive formulations in media resembling intestinal fluids: bicarbonate *versus* phosphate buffers. J Drug Deliv Sci Tech. 2005;15(4):273–9.
25. Mooney KG, Mintun MA, Himmelstein KJ, Stella VJ. Dissolution kinetics of carboxylic acids II: effect of buffers. J Pharm Sci. 1981;70(1):22–32. Epub 1981/01/01.
26. Daniels JT, Cambrey AD, Occleston NL, Garrett Q, Tarnuzzer RW, Schultz GS, *et al*. Matrix metalloproteinase inhibition modulates fibroblast-mediated matrix contraction and collagen production *in vitro*. Investig Ophthalmol Vis Sci. 2003;44(3):1104–10.
27. Fisher JF, Mobashery S. Recent advances in MMP inhibitor design. Cancer Metastasis Rev. 2006;25(1):115–36.
28. Aguiar AJ, Krc J, Kinkel AW, Samyn JC. Effect of polymorphism on absorption of chloramphenicol from chloramphenicol palmitate. J Pharm Sci. 1967;56(7):847–53.
29. Aguiar AJ, Zelmer JE. Dissolution behavior of polymorphs of chloramphenicol palmitate and mefenamic acid. J Pharm Sci. 1969;58(8):983–7.
30. Khalafallah N, Khalil SA, Moustafa MA. Bioavailability determination of 2 crystal forms of sulfameter in humans from urinary-excretion data. J Pharm Sci. 1974;63(6):861–4.